ACS OMEGA

http://pubs.acs.org/journal/acsodf

Article

Synthesis, Molecular Docking, and Biological Evaluation of a New Series of Benzothiazinones and Their Benzothiazinyl Acetate Derivatives as Anticancer Agents against MCF-7 Human Breast Cancer Cells and as Anti-Inflammatory Agents

Farhat Ramzan, Syed Ayaz Nabi, Mehak Saba Lone, Khalid Imtiyaz, Laraib Urooj, Vishakha Vishakha, Kalicharan Sharma, M. Moshahid A. Rizvi, Syed Shafi, Mohammed Samim, Sameena Bano,* and Kalim Javed*

Cite This: *ACS Omega* 2023, 8, 6650−6662

Read Online

ACCESS | Metrics & More | Article Recommendations | Supporting Information

ABSTRACT: Six 1,4-benzothiazin-3-ones (**2a−f**) and four benzothiazinyl acetate derivatives (**3a−d**) were synthesized and characterized by various spectroscopic methods, namely, ^{1}H NMR, ^{13}C NMR, IR, MS, and elemental analysis. The cytotoxic effects of the compounds were assessed against MCF-7, a human breast cancer cell line, along with their anti-inflammatory activity. Molecular docking studies performed against the VEGFR2 kinase receptor displayed a common binding orientation of the compounds in the catalytic binding pocket of the receptor. The generalized Born surface area (GBSA) studies of compound **2c** with the highest docking score also proved its stability in binding to the kinase receptor. Compounds **2c** and **2b** showed better results against VEGFR2 kinase with IC_{50} values of 0.0528 and 0.0593 μM, respectively, compared to sorafenib. All of the compounds (**2a−f** and **3a−d**) showed effective growth inhibition having (IC_{50}) values of 2.26, 1.37, 1.29, 2.30, 4.98, 3.7, 5.19, 4.50, 4.39, and 3.31 μM, respectively, against the MCF-7 cell line compared to standard 5-fluorouracil (IC_{50} = 7.79 μM). However, compound **2c** displayed remarkable cytotoxic activity (IC_{50} = 1.29 μM), suggesting it as a lead compound in the cytotoxic assay. Additionally, compounds **2c** and **2b** showed better results against VEGFR2 kinase with IC50 values of 0.0528 and 0.0593 μM, respectively, compared to sorafenib. It also inhibited hemolysis by stabilizing the membrane comparable to that of diclofenac sodium, a standard used in the human red blood cell membrane stabilization assay and hence can act as a template for designing novel anticancer and anti-inflammatory agents.

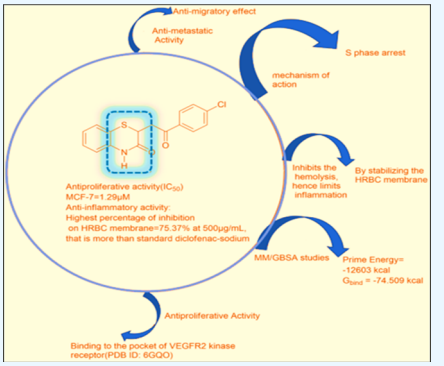

1. INTRODUCTION

Uncontrolled proliferation of some abnormal cells in the body results in a deadly growth called cancer. Viscera get damaged as these cells may spread through blood or lymph in the entire body by dividing and producing unlimited new cells.[1] Since there are multiple types of cancers present, it is therefore difficult to find a single cure for cancer.[2] It is still the second most common cause of death across the globe despite vast progress in the field of research, thus accounting for almost 13% of all deaths after cardiovascular diseases, both in developing and developed nations.[3,4] Out of these, the second major cause of death among women is breast cancer globally.[5] It affects almost 2.1 million women annually, and in 2018, almost 627,000 women died of this cancer, which is around 15% of total deaths. With a total contribution of 24.2% incidence worldwide, the rate of breast cancer is higher among women in developed regions.[6,7] Axitinib, methotrexate, raloxifene, and doxorubicin are the class of drugs used for treating breast cancer, yet the need for more potent anticancer agents cannot be ruled out.[8] On the other hand, cancer and inflammation are closely related, and many diseases caused by inflammation such as rheumatoid arthritis can be treated by various anticancer agents. Moreover, the risk for various cancers is further increased by chronic inflammation. This suggests that reducing inflammation may be a viable method of preventing and treating cancer.[9] Similarly, inflammatory conditions[10,11] such as injuries and post-operative pain although can be treated by nonsteroidal anti-inflammatory drugs (NSAIDs), their adverse effects such as gastrointestinal disorders and renal, cardiovascular, and hepatic issues[12,13] cannot be neglected; however, these adverse effects can be reduced by designing a type of effective and safe anti-

Received: November 6, 2022
Accepted: January 23, 2023
Published: February 7, 2023

https://doi.org/10.1021/acsomega.2c07153
ACS Omega 2023, 8, 6650−6662

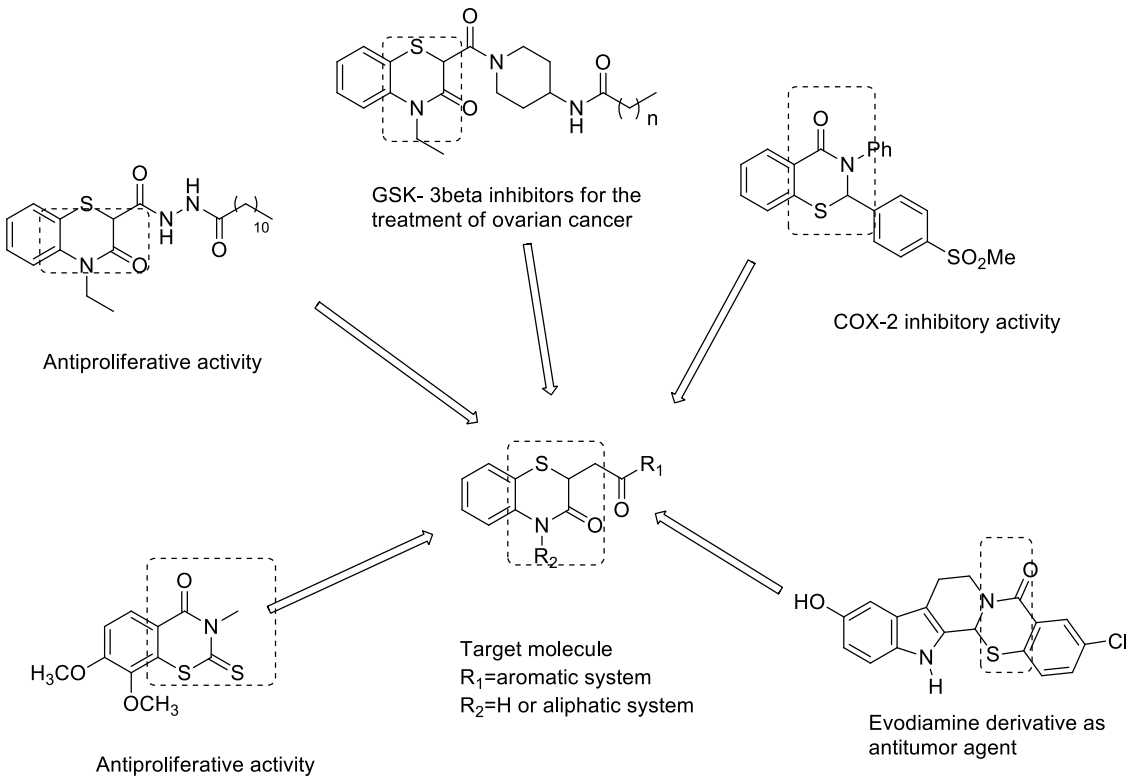

Figure 1. Structures of the compounds of biological interest, with several active benzothiazinone pharmacophores.

Scheme 1. General Procedure for the Synthesis of Benzothiazinones (2a−f) and Benzothiazinyl Acetate Derivatives (3a−d)

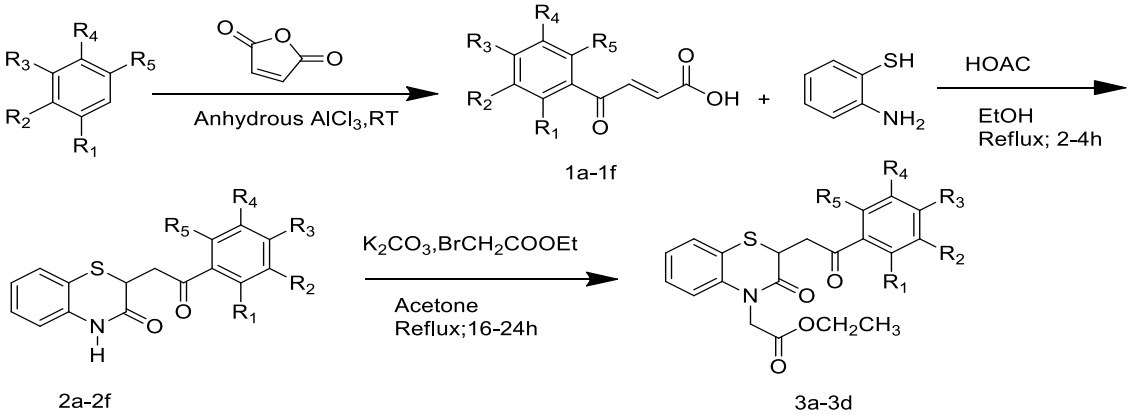

1a, 2a, 3a: R_3 =F, R_1= R_2=R_4 =R_5=H

1b, 2b, 3b: R_2 = R_3= F, R_1=R_4 =R_5=H

1c, 2c, 3c: R_3 =Cl, R_1= R_2=R_4 =R_5=H

1d, 2d, 3d: R_3 =Br, R_1= R_2=R_4 =R_5=H

1e, 2e: R_2 =R_3= Cl, R_1= R_4 =R_5=H

1f, 2f: R_2 =Cl, R_3=CH_3, R_1= R_4= R_5 =H

inflammatory and anticancer agents. Numerous studies have shown that both primary and metastatic breast cancers overexpress a number of receptor tyrosine kinases (RTKs), including the vascular endothelial growth factor receptor (VEGFR), the fibroblast growth factor receptor (FGFR), and the platelet-derived growth factor receptor (PDGFR). This then triggers tumor metastasis, angiogenesis, and carcinogenesis. One of the key routes involved in tumor angiogenesis was found to be VEGFR2. Therefore, it has long been assumed that blocking the VEGFR2 pathway would result in an effective antiangiogenic and antitumor response. Due to improved prognosis in cancer patients, several VEGFR2 targeted

https://doi.org/10.1021/acsomega.2c07153
ACS Omega 2023, 8, 6650−6662

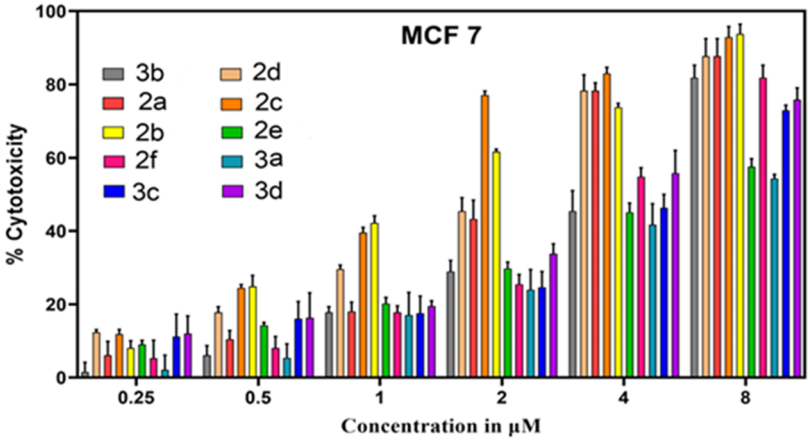

Figure 2. Concentration-dependent cytotoxic potential of compounds against the MCF-7 cell line with concentrations ranging from 0.25 to 8 μM. Mean ± S.D is indicated by the error bar.

inhibitors have been clinically authorized either alone or in combination with other chemotherapies.[14] Though much progress has been made in cancer management by chemotherapy, continuous effort to find out new anticancer and anti-inflammatory agents remains important. Benzothiazinones are a class of sulfur-containing heterocyclic compounds that display a significant role in drug discovery. Besides their antibacterial and antifungal activities,[15−19] they possess diverse biological properties including anticancer,[20−23] antituberculosis,[24] and anti-inflammatory activities.[25] The antitumor activity of many novel benzothiazinone-containing moieties has recently been reported.[26] Based on their reactivity, it is therefore possible to design and synthesize many aromatic and nonaromatic heterocyclic systems for evaluating their anticancer activity. The physicochemical properties and pharmacological activities[27,28] of drugs with heterocyclic moieties containing nitrogen are widespread. In almost 30 countries, a benzothiazionone derivative, oxicam, is used to treat both acute and chronic inflammation, whereas osteoarthritis and rheumatoid arthritis are treated by meloxicam.[29−31] Clinical trials show that they have the potential to act as novel alternatives for anti-inflammatory and anticancer drugs, deprived of the adverse effects of the currently available drugs. Hence, these studies were found to be helpful to explore the anticancer and anti-inflammatory properties of these compounds.

This study is significant, as it aims to develop benzothiazinones and their acetate derivatives as effective anticancer and anti-inflammatory drugs with more inhibition activity. Keeping in view the promising activities of benzothiazinones (Figure 1), this study focused on the benzothiazinone nucleus for exploring its potency in developing effective novel compounds. The present study describes the synthesis and structural characterization of benzothiazinones and their novel derivatives and their cytotoxic effect on the human breast cancer cell line MCF-7 as well as their anti-inflammatory action. The compounds were also assessed at the molecular level by simulation docking studies for a better understanding of their inhibitory potency as well as interaction with the active site of the VEGFR2 kinase receptor. Results obtained in this work demonstrate that these moieties curb breast cancer cell growth and hinder inflammation as well, hence opening a new approach toward utilizing these compounds in developing novel and more effective anticancer and anti-inflammatory agents.

2. RESULTS AND DISCUSSION

2.1. Chemistry. The reactions for the synthesis of titled compounds (**2a−f** and **3a−d**) are shown in Scheme 1. Benzothiazinones (**2a−f**) were synthesized through the reported method by the reaction of β-aroylacrylic acids with 2-aminothiophenol[32] and in anhydrous conditions by refluxing them in acetone with bromo-substituted ester. These were further transformed into benzothiazinyl acetate derivatives. β-Aroylacrylic acids (**1a−f**) needed for the synthesis of benzothiazinones were obtained by Friedel Crafts acylation.[33,34] The ^{1}H NMR spectra of the compounds were generally clean, and all compounds could be described as being >95% pure by ^{1}H NMR. Earlier, Beryozkina and co-workers reported the synthesis of **2a**, **2b**, **2c**, and **2d**. However, the biological evaluation of these compounds has not been reported.[32]

The structures of compounds were confirmed by spectroscopic methods such as IR, MS, ^{1}H NMR, ^{13}C NMR, and elemental analysis. For benzothiazinyl acetate derivatives (**3a−d**), characteristic bands in the IR were noticed at 1680−1670 for the carbonyl group (C═O), 1740−1732 for the carbonyl group (C═O) of ester, and 3459−3450 for the association of the amide-linked carbonyl group (C═O). In the ^{1}H NMR spectra of these acetate derivatives, a sharp triplet appeared at δ = 1.2−1.29 ppm for ($COOCH_2CH_3$) protons and a quartet at δ = 4.67 ppm for ($COOCH_2CH_3$) protons. They also showed a group of signals with two doublets of doublets for the ($-CH_2$) unit at δ = 3.15−3.75 ppm and a triplet for the (−CH) proton at δ = 4.20−4.23 ppm. A sharp singlet appeared at 4.26−4.28 for two protons of the ($CH_2COOCH_2CH_3$) unit. Aromatic ring protons were observed at 6.92−7.99 ppm. A sharp singlet for the NH group proton was recorded at 10.71−10.72 in the ^{1}H NMR spectra of benzothiazinones and a typical ABX structure because of the CH−CH_2 protons. All other peaks in ^{13}C NMR were noticed at expected ppms. In the ^{13}C NMR spectra of compounds **3a** and **3b**, splitting was observed with the expected number of ^{13}C signals. Compound **3a**, with one fluorine, showed 3 C's with doublets with different J values. For compound **3b**, with adjacent fluorines on a benzene ring, there were doublets of doublets present in the ^{13}C NMR. In

https://doi.org/10.1021/acsomega.2c07153
ACS Omega 2023, 8, 6650−6662

the MS spectral data of the compounds, M + 2 peaks correspond to isotopes of ^{81}Br and ^{37}Cl isotopes. Mass, ^{1}H NMR, and ^{13}C of the spectra of all compounds are given in the Supporting Information (SI).

2.2. Biological Evaluation. *2.2.1. In Vitro Antiproliferative Activity (MTT Assay).* The MTT in vitro cell proliferation assay is one of the most commonly used assays for the preliminary evaluation of the anticancer activity of various compounds.[35,36] The cytotoxicity of synthesized compounds was evaluated against the human MCF-7 cell line via the MTT assay. The effectiveness of the compounds was estimated with serial dilutions ranging from 0.25 to 8 μM against 5-fluorouracil as a standard. It was observed that cytotoxic activity is dependent on the concentration of the compound and was found to be highest at 8 μM (Figure 2).

The IC_{50} values of these compounds were determined and are summarized in Table 1. Results indicated that all of the compounds exhibited potent cytotoxicity against tested MCF-7 cell lines. Compound **2c** was found to have significantly higher cytotoxic potential with an IC_{50} of 1.29 μM compared to the rest of the compounds of the same series. Based on these findings, compound **2c** was selected for further evaluation.

Table 1. IC_{50} Values of the Synthesized Compounds (2a−f and 3a−d) on the Human MCF-7 Cell Line

compounds	1 C_{50} (μM)
2a	2.26
2b	1.37
2c	1.29
2d	2.30
2e	4.98
2f	3.70
3a	5.19
3b	4.50
3c	4.39
3d	3.31
5-fluorouracil	7.79

2.2.1.1. Cell Cycle Analysis. Cell cycle changes were observed by staining compound **2c** for 24 h with propidium iodide using flow cytometric analysis.[37] Notable cell cycle arrest by compound **2c** was observed around the S phase at 1.29 μM concentration, and compared to that of control, the cell distribution in G0/G1 and G2/M phases remarkably decreased. There was a 1% decrease in the population of MCF-7 cells at the G2/M phase when treated with compound **2c** (1.29 μM), which was almost half in comparison to the control group (2.4%; Figure 3). The treatment of compound **2c** with MCF-7 cells showed 76.2 and 22.7% population of cells at G0/G1 and S phases, respectively, whereas in untreated control, 88.2 and 9.4% of cells were present, respectively. The cell percentage in the S phase increased in comparison to the control, whereas at G0/G1 and G2/M phases, the population decreased. This shows that cell division and cell proliferation of MCF-7 cells are inhibited by compound **2c** in the S phase of the cell cycle. (Figure 3)

2.2.1.2. Wound Healing Assay. The antimetastatic effect for compound **2c** was observed by the wound healing or cell scratching method. It is done by taking the images at various intervals after a wound has been created on a confluent cell monolayer. The pace of migration of cancer cells can be assessed by capturing the images both at the beginning and at various intervals of migration of cells. In cancer metastasis, it is an important process because cells migrate to reinstate the interaction at the scratched edges and try to fill the wound after the wound is created artificially.[38] In the wound area of the cells treated with compound **2c**, significant inhibition in the cell migration was observed because of the antimetastatic effect of the compound, whereas cells healed the wound area by migrating to scratched edges in that of the control group, where no treatment was given. The area between the edges was

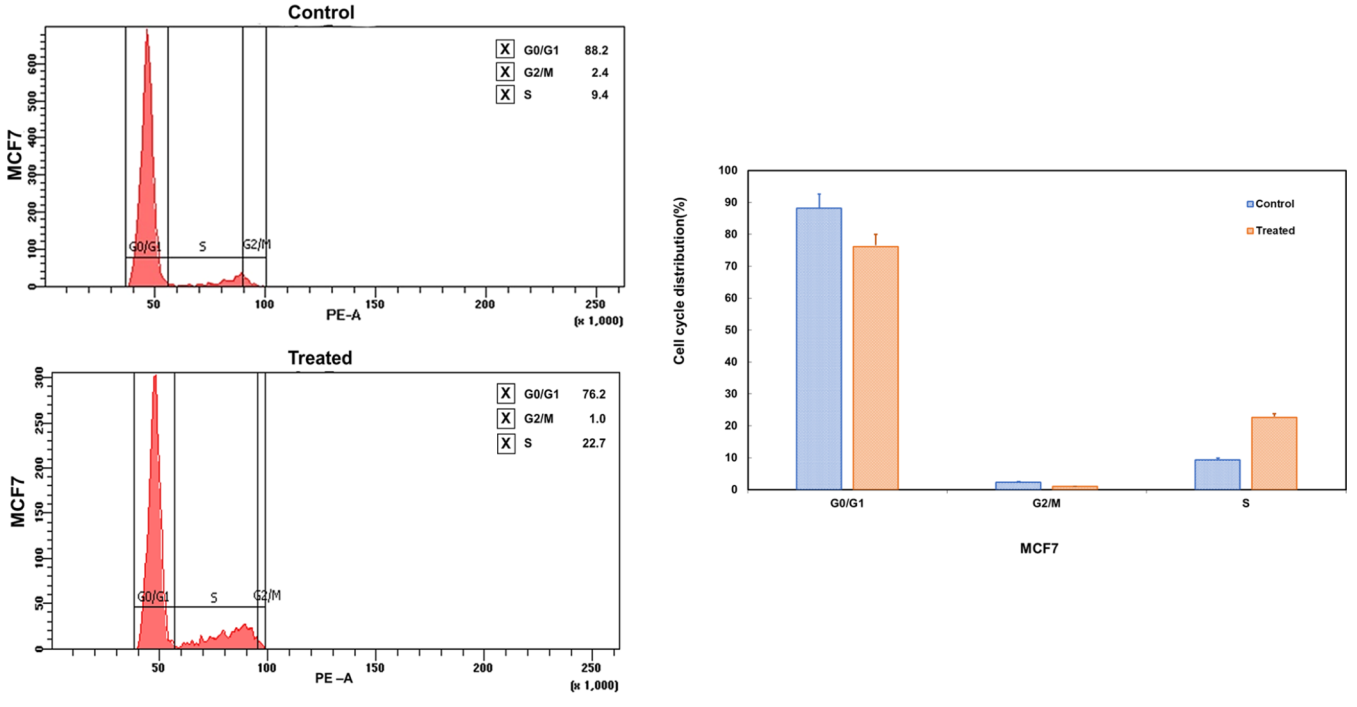

Figure 3. Induction of S phase cell cycle arrest by compound **2c** in MCF-7 treated cells compared with control cells.

https://doi.org/10.1021/acsomega.2c07153
ACS Omega 2023, 8, 6650−6662

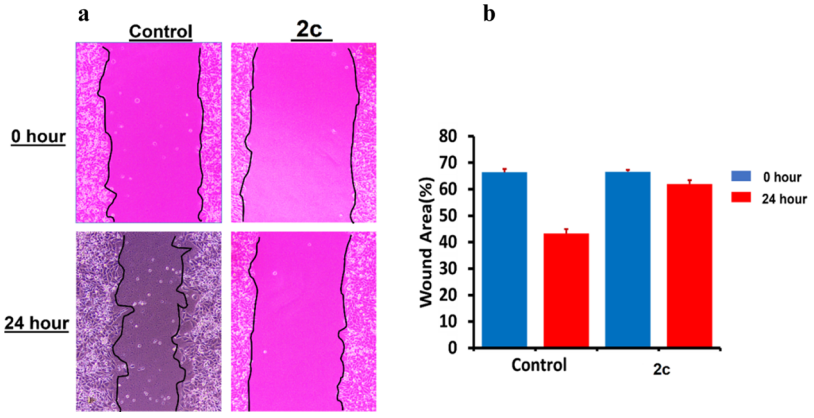

Figure 4. (a) Microscopy image shows cell migratory inhibition at 0 and 24 h for control and treated cells that depict that **2c** has more antimigratory effect than control. (b) The percentage wound healing area of control as well as **2c**-treated MCF-7 cells at 0 and 24 h.

covered almost entirely in control cells. By calculating the wound healing percentage, it was found to be 66.42 ± 1.20 for control and 66.63 ± 0.66 for treated cells at 0 h. The reduction in the area of the wound was found to be 43.23 ± 1.71 for control and 61.98 ± 1.44 for treated cells after 24 h. Thus, microscopy images (Figure 4a) show more migratory inhibition of MCF-7-treated cells than control at 24 h, and the antimigratory potential of **2c** is clearly shown in Figure 4b.

2.2.2. In Vitro VEGFR2 Kinase Assay. Compounds **2a−f** and **3a−d** were further evaluated against VEGFR2 kinase by an antiphosphotyrosine antibody with the Alpha Screen system. The obtained IC50 values are shown in Table 2. Sorafenib was used as a reference drug in this assay. It was observed that **2c** and **2b** showed better results than the reference drug, having IC_{50} values of 0.0528 and 0.0593 μM, respectively, whereas the other compounds showed IC_{50} values ranging from 0.0741 to 0.6321 μM. It is noticeable that compound **2c** is the most potent in both the antiproliferative assay and the VEGFR2 inhibition assay compared to other compounds of the series as well as sorafenib.

Table 2. In Vitro VEGFR2 Inhibitory Activity of the Compounds and Sorafenib

compound code	VEGFR2 IC_{50} (μM)
2a	0.0741
2b	0.0593
2c	0.0528
2d	0.2312
2e	0.1346
2f	0.0972
3a	0.6321
3b	0.2361
3c	0.1320
3d	0.4437
sorafenib	0.0643

2.2.3. In Vitro Anti-Inflammatory Activity. Various typical changes may happen when the lysosomal enzymes are released during inflammation.[39] Many anti-inflammatory agents limit inflammation by preventing lysosomal components and chemical mediators of activated neutrophils from releasing, thus stabilizing the lysosomal membrane.[40−42] Since the lysosomal and red blood cell membranes are almost alike, so we can extrapolate the stabilization of the erythrocyte membrane with that of lysosomal membrane stabilization. The effects of various synthesized benzothiazinones and their derivatives were evaluated on the stabilization of the human red blood cell (HRBC) membrane (Figure 5). At different concentrations, hemolysis was inhibited by all of the compounds, thus having the capability of stabilizing the red blood cell membrane in a hypotonic solution. Compound **2c** showed the highest percentages of inhibition of 31.62, 49.82, and 75.37% at concentrations of 125, 250, and 500 μg/mL, respectively, compared to the standard drug diclofenac sodium. Compound **3c** also has almost comparable percentages of inhibition of 27.35 and 53.62% at 125 and 500 μg/mL, respectively, to that of the standard. This shows that the

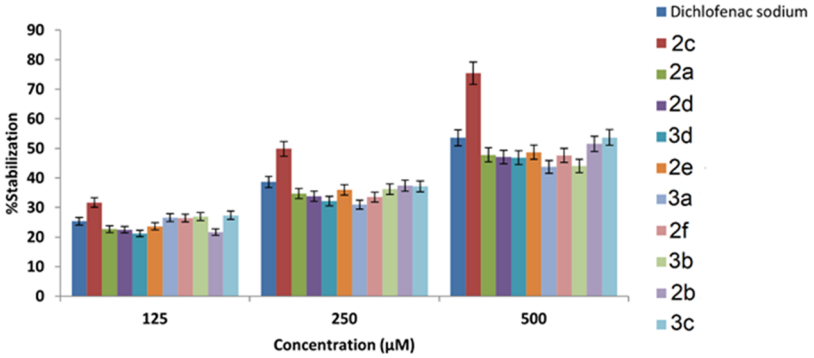

Figure 5. Percent stabilization on the HRBC membrane by benzothiazinones and their benzothiazinyl acetate derivatives using the standard drug diclofenac sodium.

https://doi.org/10.1021/acsomega.2c07153
ACS Omega 2023, 8, 6650−6662

percentage of membrane stability increases upon increasing the dose (Figure 5). However, the activity of the rest of the compounds was lower than that of the standard drug.

2.2.4. In Silico Studies. 2.2.4.1. Molecular Docking. The molecular docking of the compounds (**2a−f** and **3a−d**) was performed against the VEGFR2 kinase receptor (Homo sapiens), and a common binding mode of compounds in the binding pocket of the VEGFR2 receptor with PDB ID(6GQO) was revealed by the docking studies (Table 3).[43,44] The pose of the binding mode of the compounds (**2a−f** and **3a−d**) was compared with the standard ligand (F82) bonded to the receptor protein (Figure 6a,b). All compounds bind to the receptor in inactive DFG-Out confirmation (Type II). It seems that the molecular docking scores in Table 2 values generally track well with the observed IC_{50} values in Table 1. Compound **2c**, with the highest docking score, showed good binding interaction with the backbone of the VEGFR2 kinase receptor by having favorable hydrophobic interaction with GLU885, GLU917, ASP1046, pi−pi stacking with LYS868, and hydrogen bonding interaction with CYS 919, which constitutes an important residue in catalysis and binding (Figure 7a,b). A similar interaction was shown by compound **2c** in the catalytic domain of the VEGFR2 kinase receptor upon superimposition with the co-crystal ligand (F82-2-(4-((6,7-dimethoxyquinazolin-4-yl)oxy)-2-methoxyphenyl)-*N*-(1-isopropyl-1*H*-pyrazol-4-yl)acetamide; Figure 8).

Table 3. Molecular Docking Score Results of All Compounds at the Active Site of the VEGFR2 Kinase Receptor

ligand	docking score (Kcal/mol)
2a	−6.79
2b	−7.34
2c	−7.47
2d	−7.01
2e	−6.71
2f	−7.22
3a	−6.24
3b	−6.98
3c	−5.62
3d	−6.09
F82 (cocrystallized ligand)	−13.70

2.2.4.2. GBSA/MM Study. The generalized Born surface area/molecular mechanics (GBSA/MM) analysis of the most potent compound **2c** with 6GQO was performed to evaluate ligand stability in the binding pocket of the VEGFR2 receptor. The results show that the prime energy and free energy of binding (ΔG_{bind}) of compound **2c** was approx. −12,603 (Kcal/mol) and −74.509 (Kcal/mol), respectively, whereas the prime energy and binding free energy of the standard cocrystallized ligand to the VEGFR2 kinase receptor (PDB ID: 6GQO) were found to be −12,712 (Kcal/mol) and −104.112 (Kcal/mol) respectively, indicating that the energy of binding of compound **2c** with the VEGFR2 kinase receptor is comparable to that of the cocrystallized ligand, hence leading to its stability in binding to the receptor (Table 4).

3. CONCLUSIONS

In the present study, the structures of synthesized six benzothiazinones and four new benzothiazinyl acetate derivatives were supported by spectroscopic data and elemental analysis. All of the synthesized compounds have higher cytotoxic activity than standard 5-fluorouracil for inhibiting the proliferation of cells against breast cancer, i.e., MCF-7 cell line, while **2c** was found to have significantly more cytotoxic potential. The mechanism of action for its cytotoxic activity may be due to the stimulation of cell cycle arrest at the S phase. The wound healing assay reveals the antimetastatic potential of compound **2c** by hindering the migration of MCF-7 cells. Compounds **2c** and **2b** showed better results against VEGFR2 kinase when compared with the reference drug, sorafenib, having IC_{50} values of 0.0528 and 0.0593 μM, respectively. Moreover, it was found that all compounds inhibited hemolysis at different concentrations by stabilizing the RBC membrane in a hypotonic solution, hence reducing inflammation. Compound **2c** showed the highest percentage of inhibition of hemolysis than the standard drug diclofenac sodium. Docking score and molecular interaction studies support the antiproliferative activity of compound **2c** and reveal a good picture of the compound's affinity and fit inside the catalytic binding pocket of the VEGFR2 kinase receptor,

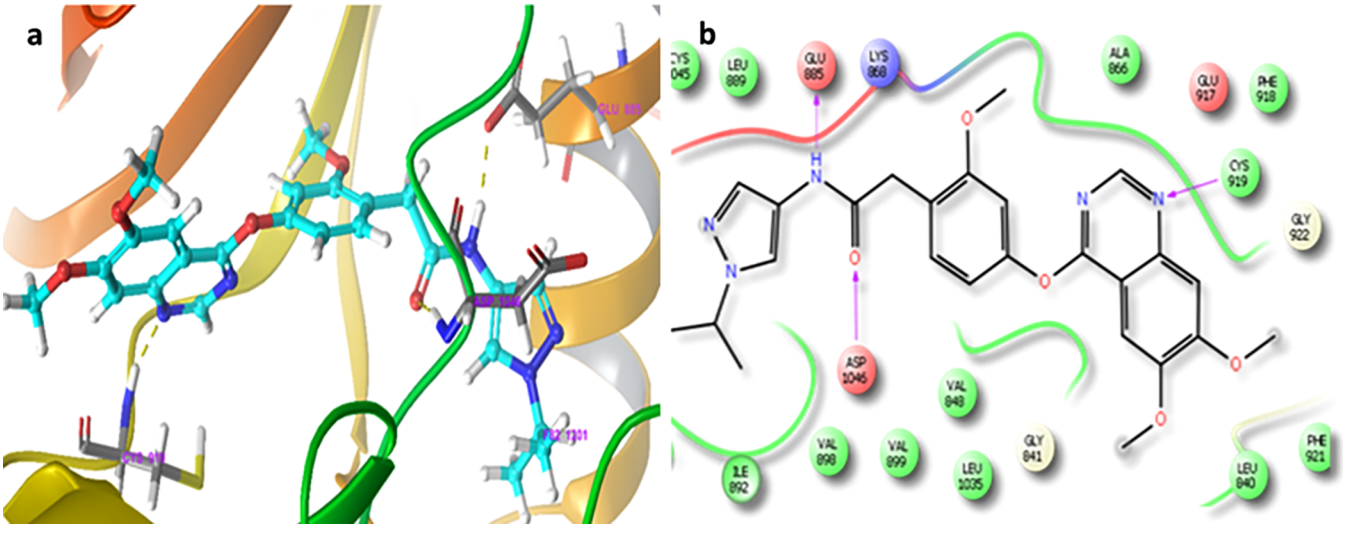

Figure 6. (a) Binding mode of the co-crystal ligand (F82) in the VEGFR2 kinase receptor. (b) 2D interaction diagram.

https://doi.org/10.1021/acsomega.2c07153
ACS Omega 2023, 8, 6650−6662

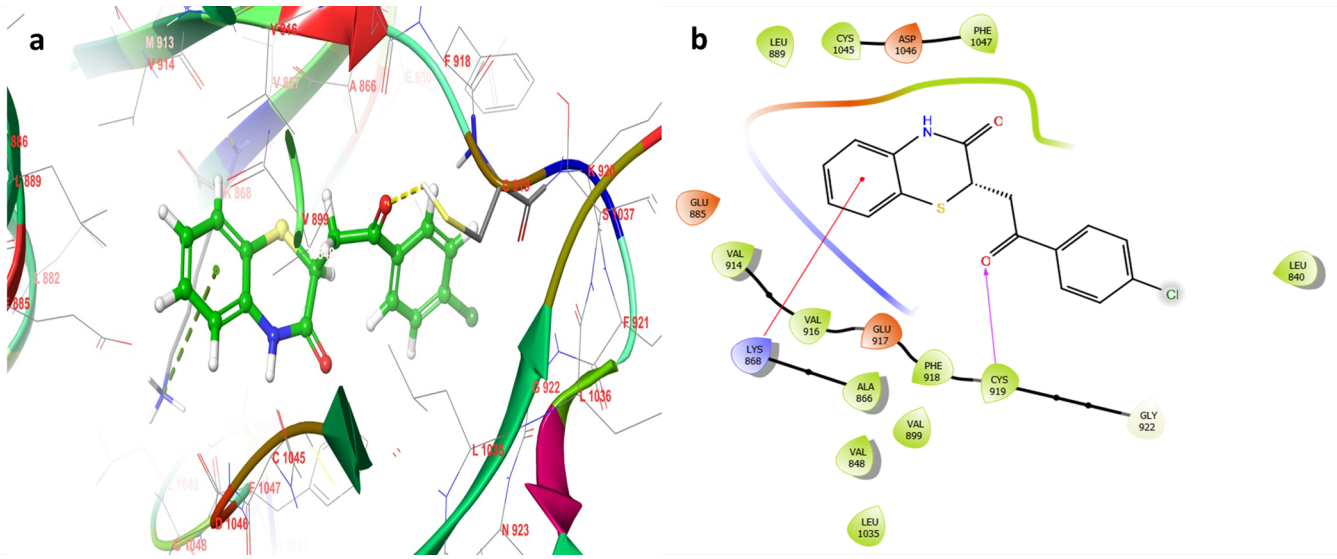

Figure 7. (a) Binding mode of highest-docking-score compound **2c** in the VEGFR2 kinase receptor (PDB ID:6GQO) active site. (b) 2D interaction of compound **2c** with the ligand.

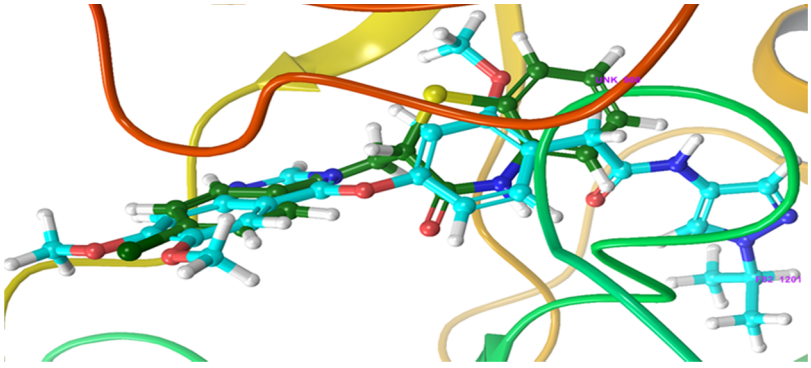

Figure 8. Superimposition of compound **2c** (yellow) with the co-crystal ligand F82 (brown) at the catalytic domain of the VEGFR2 kinase receptor (PDB ID: 6GQO).

Table 4. GBSA/MM Value of the Active Most Compound 2c and the Standard Cocrystallized Compound (F82) in the VEGFR2 Receptor (PDB ID: 6GQO)

s.no	compound	prime energy (Kcal/mol)	ΔG_{bind} (Kcal/mol)
1	**2c**	−12,603	−74.509
2	F82 (cocrystalized ligand)	−12,712	−104.112

which is further supported by the MM/GBSA study. On the basis of the results of in vitro and in silico studies, we present compound **2c** as a template for designing novel anticancer and anti-inflammatory agents.

4. METHODS

4.1. Chemistry. Chemicals of analytical grade, used as reagents and starting materials, were procured from Sigma-Aldrich, Merck (Germany), and Spectrochem. Open capillary tubes were used to determine melting points and were uncorrected. A BIO-RAD FTS-135 spectrophotometer (Waltham, MA) was used to record Fourier transform infrared (FTIR) by making the use of KBr pellets, and ν_{max} values were given in cm^{-1}. A Bruker Spectrospin DPX 500 MHz spectrometer (Fallanden, Switzerland) was used to record ^1H NMR spectra by tetramethylsilane (TMS) as an internal standard and $CDCl_3$ or (DMSO-d_6) as the solvent. J values, i.e., coupling constants, are expressed in Hertz, and chemical shift values are given in the δ (ppm) scale. A Bruker Spectrospin DPX at 125 MHz was used to record ^{13}C spectra. Managed by mass lynx software (version 4.1), a XEVO TQ-S triple quadruple mass spectrometer (Waters) was used to scan mass spectra (MS), and more intense peak values were specified by the m/z ratio. TLC plates (silica gel G) were utilized for determining the purity of the compounds, and further visualization was done by exposing them to vapors of iodine. To carry out elemental analysis, a CHNS Elementar (Vario EL III, Hanau Germany) was used. ^1H NMR and mass spectra of all compounds and ^{13}C spectra of some compounds are given in Supporting Information.

4.2. General Procedure for the Synthesis of Aroylacrylic Acids (1a−f). Aluminum chloride anhydrous (0.125 mol, 16.6 g) was mixed with 30 mL of liquid hydrocarbon of aromatic nature. The mixture was stirred with a magnetic stirrer for half an hour at room temperature. Maleic anhydride (0.05 mol, 5 g), in five portions, was added with continuous stirring. Stirring was maintained at room temperature for the next 6 h. The mixture was kept at room temperature for the next 48 h, followed by the addition of

https://doi.org/10.1021/acsomega.2c07153
ACS Omega 2023, 8, 6650−6662

chilled hydrochloric acid (50%, 100 mL). To remove the excess solvent, steam distillation was carried out. The precipitate was treated with an aqueous saturated sodium bicarbonate solution and then filtered. Dilute HCl (4% v/v) was used to acidify the filtrate. The precipitate was filtered, washed with cold water, and then dried. The precipitate was crystallized using the appropriate solvent to obtain compounds (**1a−f**). For determining the purity of the compounds, a formic acid/ethyl acetate/toluene (1:4:5) solvent system was used.

4.3. General Procedure for the Synthesis of 1,4-Benzothiazinones (2a−f). An appropriate mixture of *β*-aroylacrylic acid **1a−f** (3 mmol), 2-aminothiophenol (3 mmol), and glacial acetic acid (0.7 mL) was refluxed in absolute ethanol (10−20 mL) for 2−4 h. The precipitate was then crystallized by an appropriate solvent to obtain pure compounds (**2a−f**). A solvent system [ethyl acetate/toluene/petroleum ether; 3:5:10] was used to determine the purity of the compounds.

4.3.1. 2-(2-(4-Fluorophenyl)-2-oxoethyl)-2H-benzo[b]-[1,4]thiazin-3(4H)-one ***2a***. Yield (97%); an off-white crystalline solid compound; m.p. 174−175 °C; R_f = 0.68 [ethyl acetate/toluene/petroleum ether; 3:5:10]. FTIR (KBr), ν (cm^{-1}): 1653 (C═O), 3049 (NH−CO). ^{1}H NMR (400 MHz, DMSO-d_6,δ):3.26 (dd, 1*H*, CHA, JAB = 17.6 Hz, JAX = 6.8 Hz), 3.70 (dd, 1*H*, CHB, JBA = 17.6 Hz, JBX = 6.8 Hz), 4.067 (t, 1*H*, CHX, *J* = 6.8 Hz), 6.9−7.03 (m, 2*H*, H8, H10, aromatic ring), 7.20 (t, 1*H*, aromatic ring), 7.24−8.09 (m, 5*H*, aromatic protons), 10.72 (s, 1*H*, NH). ^{13}C NMR (125 MHz, DMSO-d_6, δ, ppm): δ = 37.14, δ = 37.60, δ = 116.30 (d, 2JC-F = 21 Hz), δ = 117.76, δ = 119.42 δ = 123.59, δ = 127.78, δ = 128.04,δ = 131.71 (d, 3JC-F = 10 Hz), δ = 133.43, δ = 137.54, δ = 165.71 (d, 1JC-F = 251 Hz), δ = 166.53, δ = 195.15. FAB-MS (*m*/*z*): 301 [M^+], 302 [M^+ + 1]. Molecular formula calculation was based on elemental analysis for $C_{16}H_{12}FNO_2S$: C = 63.77, H = 4.01, F = 6.30, N = 4.65, O = 10.62, S = 10.64. Found: C = 63.74, H = 4.05, F = 6.60, N = 4.55, O = 10.64, S = 10.44.

4.3.2. 2-(2-(3, 4-Difluorophenyl)-2-oxoethyl)-2H-benzo[b]-[1,4]thiazin-3(4H)-one ***2b***. Yield (95%); an off-white crystalline solid compound; m.p. 192−193.5 °C; R_f = 0.65 [ethyl acetate/toluene/petroleum ether; 3:5:10]. FTIR (KBr), ν (cm^{-1}): 1653 (C═O), 3049 (NH−CO). ^{1}H NMR (300 MHz, DMSO-d_6, δ): 3.28 (dd, 1*H*, CHA, JAB = 17.7 Hz, JAX = 6.3 Hz), 3.72 (dd, 1*H*, CHB, JBA = 17.7 Hz, JBX = 6.9 Hz), 4.069 (t, 1*H*, CHX, *J* = 6.6 Hz), 6.97−7.03 (m, 2*H*, aromatic protons), 7.2 (t, 1*H*, aromatic), 7.32 (d, 1*H*, aromatic ring), 7.5−8.08 (m, 3*H*, aromatic ring), 10.71 (s, 1*H*, NH). ^{13}C NMR (125 MHz, DMSO-d_6, δ, ppm): δ = 37.13, δ = 37.69, δ = 117.77, δ = 118.30 (dd, 2JC-F = 43 Hz, 3JC-F = 18 Hz), δ = 119.40, δ = 123.60, δ = 126.53 (dd, 2JC-F = 9 Hz, 3JC-F = 4 Hz), δ = 127.80, δ = 128.03, δ = 134.11, δ = 134.27, δ = 137.52, δ = 150.01 (dd, 1JC-F = 246 Hz, 2JC-F = 13 Hz), δ = 153.25 (dd, 1JC-F = 240 Hz, 2JC-F = 12 Hz), δ = 166.15, δ = 194.75. FAB-MS (*m*/*z*): 319 [M^+], 320 [M^+ + 1]. Molecular formula calculation was based on elemental analysis for $C_{16}H_{11}F_2NO_2S$: C = 60.18 H = 3.47, F = 11.90, N = 4.39, O = 10.02, S = 10.04. Found: C = 60.20, H = 3.48, F = 11.84, N = 4.36,O = 10.01, S = 10.08.

4.3.3. 2-(2-(4-Chlorophenyl)-2-oxoethyl)-2H-benzo[b] [1, 4]thiazin-3(4H)-one ***2c***. Yield 98%; a white crystalline solid compound; m.p. = 197−198 °C; R_f = 0.64 [ethyl acetate/toluene/petroleum ether; 3:5:10]. FTIR (KBr), v_{max} cm^{-1}: 1653 (C═O), 3061(NH). ^{1}H NMR (500 MHz DMSO-d_6,δ):3.27 (dd, 1*H*, CHA, JAB = 17.5 Hz, JAX = 6.5 Hz), 3.71 (dd, 1*H*, CHB, JBA = 17.5 Hz, JBX = 6.5 Hz), 4.07 (t, 1*H*, CHX, *J* = 6.75 Hz), 6.9−7.01 (m, 2*H*, aromatic ring), 7.24 (t, 1*H*, aromatic ring), 7.31−7.37 (m, 3*H*, aromatic ring), 8.07−8.10 (m, 2*H*, aromatic ring), 10.74 (s, 1*H*, NH). ^{13}C NMR (125 MHz, DMSO -d_6, δ,ppm): δ = 37.11, δ = 37.57, δ = 116.15, δ = 116.33, δ = 117.73, δ = 119.35 δ = 123.5(2C), δ = 127.71, 127.98(2C), δ = 133.36, δ = 133.38, δ = 137.50, δ = 166.47, δ = 195.17. FAB-MS (*m*/*z*): 317 [M^+], 318 [M^+ + 1], 319 [M^+ + 2], 320 [M^+ + 3]. Molecular formula calculation was based on elemental analysis for the $C_{16}H_{12}ClNO_2S$: C = 60.47, H = 3.81, Cl = 11.16, N = 4.41,O = 10.07, S = 10.09. Found: C = 60.14, H = 3.70, Cl = 11.27, N = 4.32, O = 10.06,S = 10.08.

4.3.4. 2-(2-(4-Bromophenyl)-2-oxoethyl)-2H-benzo[b]-[1,4]thiazin-3(4H)-one ***2d***. Yield 95%; a white crystalline solid compound; m.p. 193−194 °C; R_f = 0.53 [ethyl acetate/toluene/petroleum ether; 3:5:10]. FTIR (KBr), ν (cm^{-1}): 1663 (C═O), 3064 (NH−CO). ^{1}H NMR (400 MHz DMSO-d_6, δ): 3.27 (dd, 1*H*, CHA, JAB = 17.6 Hz, JAX = 6.6 Hz), 3.71 (dd, 1*H*, CHB, JBA = 17.6 Hz, JBX = 6.8 Hz), 4.076 (t, 1*H*, CHX, *J* = 6.8 Hz), 6.9−7.03 (m, 2*H*, aromatic ring), 7.23 (t, 1*H*, aromatic), 7.32 (d, 1*H*, *J* = 7.6 Hz), 7.51−8.0 (m, 4*H*, aromatic), 10.71 (s, 1*H*, NH). ^{13}C NMR (100 MHz, DMSO-d_6, δ, ppm): δ = 37.13, δ = 37.65, δ = 117.76, δ = 119.41, δ = 123.61, δ = 127.79 δ = 128.05, δ = 129.40(2C), 130.59(2C), δ = 135.52, δ = 137.52, δ = 138.96, δ = 166.50, δ = 195.70 FAB-MS (*m*/*z*): 362 [M^+], 363 [M^+ + 1], 364 [M^+ + 2]. Molecular formula calculation was based on elemental analysis for $C_{16}H_{12}BrNO_2S$: C = 53.05, H = 3.34, Br = 22.06, N = 3.87, O = 8.83, S = 8.85. Found: C = 53.05, H = 3.33, Br = 22.07, N = 3.89,O = 8.84, S = 8.88.

4.3.5. 2-(2-(3,4-Dichlorophenyl)-2-oxoethyl)-2H-benzo[b]-[1,4]thiazin-3(4H)-one ***2e***. Yield 98%; a white crystalline solid compound; m.p. 193.7−194.7 °C; R_f = 0.58 [ethyl acetate/toluene/petroleum ether; 3:5:10]. FT R (KBr), ν (cm^{-1}): 1668 (C═O), 3079 (NH−CO). ^{1}H NMR (300 MHz, DMSO-d_6, δ): 3.28 (dd, 1*H*, CHA, JAB = 17.7 Hz, JAX = 6.3 Hz), 3.72 (dd, 1*H*, CHB, JBA = 17.7 Hz, JBX = 6.9 Hz), 4.069 (t, 1*H*, CHX, *J* = 6.6 Hz), 6.97−7.03 (m, 2*H*, aromatic protons), 7.2 (t, 1*H*, aromatic), 7.32 (d, 1*H*, aromatic ring, *J* = 6.9), 7.5−8.0 (m, 3*H*, aromatic), 10.71 (s, 1*H*, NH). ^{13}C NMR (125 MHz, DMSO -d_6, δ, ppm): δ = 37.19, δ = 37.67, δ = 116.16, δ = 116.33, δ = 117.80, δ = 119.36, δ = 123.47, δ = 127.71, 127.98, δ = 131.61, δ = 131.68, δ = 133.37, δ = 133.39, δ = 137.50, δ = 166.66, δ = 195.50. FAB-MS (*m*/*z*): 352 [M^+], 353 [M^+ + 1], 354 [M^+ + 2]. Molecular formula calculation was based on elemental analysis for $C_{16}H_{11}Cl_2NO_2S$: C = 54.56, H = 3.15, Cl = 20.13, N, = 3.98, O = 9.08, S = 9.10. Found: C = 54.46, H = 3.05, Cl = 20.43, N = 3.68, O = 9.01, S = 9.14.

4.3.6. 2-(2-(3-Chloro-4-methylphenyl)-2-oxoethyl)-2H-benzo[b][1,4]thiazin-3(4H)-one ***2f***. Yield 98%, a white crystalline solid compound; m.p. 189. 6−190.6 °C, R_f = 0.59 [ethyl acetate/toluene/petroleum ether; 3:5:10]. IR (KBr), ν (cm^{-1}): 1653 (C═O), 3179 (NH−CO). ^{1}H NMR (500 MHz DMSO-d_6,δ): 2.39 (s, 3*H*, $-CH_3$), 3.25 (dd, 1*H*, CHA, JAB = 17.5 Hz, JAX = 6.5 Hz), 3.70 (dd, 1*H*, CHB, JBA = 17.5 Hz, JBX = 7 Hz), 4.07 (t, 1*H*, CHX, *J* = 6.5 Hz), 6.98−7.04 (m, 2*H*, aromatic ring), 7.20−7.32 (m, 2*H*, aromatic ring), 7.54 (d, IH, aromatic ring), 7.83 (d, IH, aromatic), 7.97(d, IH, aromatic), 10.72 (s, 1*H*, NH). ^{13}C NMR (125 MHz, DMSO -d_6, δ, ppm): δ = 19.97, δ = 37.11, δ = 37.6, δ = 117.71, δ =

https://doi.org/10.1021/acsomega.2c07153
ACS Omega 2023, 8, 6650−6662

119.32, δ = 123.54, δ = 127.71, δ = 127.99, δ = 129.73, δ = 131.36, δ = 135.34, δ = 136.64, δ = 137.47, δ = 139.13, δ = 141.94, δ = 166.45, δ = 195.76. FAB-MS (*m*/*z*): 331 [M^+], 333 [M^+ + 2], 334 [M^+ + 3.] Molecular formula calculation was based on elemental analysis for the $C_{17}H_{14}ClNO_2S$: C = 61.53, H = 4.25, Cl = 10.68, N = 4.22, O = 9.64, S = 9.66. Found: C = 61.43, H = 4.35, Cl = 10.78, N = 4.62, O = 9.24, S = 9.46.

4.4. General Procedure for the Synthesis of 1,4-Benzothiazin-4-yl Acetates (3a−d). The mixture of appropriate benzothiazinone (0.75 mmol), k_2CO_3 (313 mg, 12.3 mmol) and ethyl bromoacetate (1.5 mmol) was dissolved in dry acetone (10−20 mL) and refluxed for 16−24 h. The steam distillation process was used to remove the excess solvent, and the mixture was acidified using dilute acetic acid by pouring it on crushed ice. A column of silica gel eluted with acetone and petroleum ether was used for chromatographic purification. A solvent system, i.e., ethyl acetate/toluene/petroleum ether (3:5:10), was used to determine the purity of compounds.

4.4.1. Ethyl 2-(2-(2-(4-Fluorophenyl)-2-oxoethyl)-3-oxo-2H-benzo[b][1,4]thiazin-4(3H)-yl)acetate ***3a***. Yield 98%; an off-white crystalline solid compound; m.p. 158−159 °C; R_f = 0.88, solvent system: [ethyl acetate/ toluene/petroleum ether; 3:5:10]. FTIR (KBr), ν (cm^{-1}): 1670 (C═O of carbonyl group), 1734 (C═O of ester), 3450 (C═O) association of the amide-linked carbonyl group. ^{1}H NMR (500 MHz, $CDCl_3$, δ): 1.27 (t, 3*H*, $-COOCH_2CH_3$), 3.16 (dd, 1*H*, CHA, JAB = 17.5 Hz, JAX = 7 Hz), 3.75 (dd, 1*H*, CHB, JBA = 17.5 Hz, JBX = 6 Hz), 4.2 (t, 1*H*, CHX), 4.28 (S, 2*H*, $-CH_2$), 4.67 (q, 2*H*, $-COOCH_2CH_3$), 6.92 (d, 1*H*, arom), 7.05 (t, 1*H*, arom), 7.10−7.27 (m, 3*H*, arom ring), 7.3 (d, 1*H*, aromatic), 7.96−7.99 (2*H*, m, aromatic). ^{13}C NMR (125 MHz, $CDCl_3$ -d_6, δ, ppm): δ = 14.12, δ = 37.19, δ = 38.04, 47.52, δ = 61.58, δ = 115.82 (d, 2JC-F = 22.5 Hz), δ = 117.29, δ = 122.92, δ = 124.05, δ = 127.70, δ = 128.89, δ = 130.94(d, 3JC-F = 10 Hz), δ = 132.84, δ = 139.07, δ = 165.97(d, 1JC-F = 253 Hz), δ = 167.30, δ = 168.48, δ = 194.23. FAB-MS(*m*/*z*): 387 [M^+], 388 [M^+ + 1]. Molecular formula calculation was based on elemental analysis for $C_{20}H_{18}FNO_4S$: C = 62.00, H = 4.68, F = 4.90, N = 3.62, O = 16.52, S = 8.28. Found: C = 62.14, H = 4.48, F = 4.75, N = 3.12, O = 16.02, S = 8.48.

4.4.2. Ethyl 2-(2-(2-(3,4-Difluorophenyl)-2-oxoethyl)-3-oxo-2H-benzo [b][1,4]thiazin-4 (3H)-yl)acetate ***3b***. Yield 98%; a white crystalline solid compound; m.p. 110−111 °C; R_f = 0.82 [ethyl acetate/toluene/petroleum ether; 3:5:10]. FTIR (KBr), ν (cm^{-1}): 1680 (C═O of carbonyl group), 1740 (C═O ester), 3459 (C═O) association of the amide-linked carbonyl group. ^{1}H NMR (500 MHz, $CDCl_3$, δ): 1.27 (t, 3*H*, $-COOCH_2CH_3$), 3.12 (dd, 1*H*, CHA, JAB = 17.5 Hz, JAX = 7 Hz), 3.73 (dd, 1*H*, CHB, JBA = 17.5 Hz, JBX = 6.5 Hz), 4.20 (t, 1*H*, CHX), 4.26 (S, 2*H*, $-CH_2$), 4.67 (q, 2*H*, $-COOCH_2CH_3$), 6.92 (d, 1*H*, arom), 7.06 (t, 1*H*, arom), 7.21−7.28 (m, 2*H*, arom ring), 7.37 (d, 1*H*, arom), 7.7 (d, 1*H*, aromatic), 7.8 (t, 1*H*, aromatic). ^{13}C NMR (125 MHz, $CDCl_3$ -d_6, δ, ppm): δ = 14.04, δ = 37.17, δ = 38.16, 47.54, δ = 61.79, δ = 117.30, δ = 117.7 (dd, 2JC-F = 43.75 Hz, 3JC-F = 18.75 Hz), δ = 122.84, δ = 124.08(2C), δ = 125.30 (dd, 2JC-F = 7.5 Hz, 3JC-F = 3.75 Hz), δ = 127.74, δ = 128.86, δ = 133.52, δ = 139.05, δ = 150.44 (dd, 1JC-F = 247 Hz, 3JC-F = 12.5 Hz), δ = 153.85 (dd, 1JC-F = 255 Hz, 3JC-F = 12.5 Hz) δ = 166.95, δ = 168.22, δ = 193.56. FAB-MS (*m*/*z*): 405 [M^+], 406 [M^+ + 1]. Molecular formula calculation was based on elemental analysis for the $C_{20}H_{17}F_2NO_4S$: C = 59.25, H = 4.23, F = 9.37, N = 3.45, O = 15.79, S = 7.91. Found: C = 59.15, H = 4.03, F = 9.47, N = 3.35, O = 15.28, S = 7.64.

4.4.3. Ethyl 2-(2-(2-(4-Chlorophenyl)-2-oxoethyl)-3-oxo-2H-benzo[b][1,4]thiazin-4(3H)-yl)acetate ***3c***. Yield 98%; a white crystalline solid compound; m.p. 111−112 °C; R_f = 0.86 [ethyl acetate/toluene/petroleum ether; 3:5:10]. IR (KBr), ν (cm^{-1}): 1670 (C═O of carbonyl group), 1732 (C═O ester), 3459 (C═O) association of the amide-linked carbonyl group. ^{1}H NMR (300 MHz, $CDCl_3$, δ): 1.2 (t, 3*H*, $-COOCH_2CH_3$), 3.15 (dd, 1*H*, CHA, JAB = 17.7 Hz, JAX = 7.2 Hz), 3.75 (dd, 1*H*, CHB, JBA = 17.7 Hz, JBX = 5.7 Hz), 4.2 (t, 1*H*, CHX), 4.28 (S, 2*H*, $-CH_2$), 4.6 (q, 2*H*, $-COOCH_2CH_3$) 6.92 (d, 1*H*, aromatic), 7.05 (t, 1*H*, aromatic), 7.26 (t, 1*H*, aromatic ring), 7.36−7.44 (m, 3*H*, aromatic), 7.89 (d, 2*H*, aromatic). ^{13}C NMR (100 MHz, $CDCl_3$ -d_6, δ, ppm): δ = 14.21, δ = 37.30, δ = 38.08, 47.61, δ = 61.81, δ = 117.36,δ = 122.94, δ = 124.12, δ = 127.79, δ = 128.97, δ = 129.08(2C), δ = 129.74(2C), δ = 134.75, δ = 139.13, δ = 140.04, δ = 167.30, δ = 168.50, δ = 194.67. FAB-MS(*m*/*z*): 403 [M^+], 404 [M^+ + 1]. Molecular formula calculation was based on elemental analysis for the $C_{20}H_{18}ClNO_4S$: C = 59.48, H = 4.49, Cl = 8.78, N = 3.47, O = 15.85, S = 7.94. Found: C = 59.38, H = 4.59, Cl = 8.88, N = 3.37, O = 15.75, S = 7.88

4.4.4. Ethyl 2-(2-(2-(4-Bromophenyl)-2-oxoethyl)-3-oxo-2H-benzo[b][1,4]thiazin-4(3H)-yl)acetate ***3d***. Yield 98%; a white crystalline solid compound; m.p. 109−110 °C; R_f = 0.73 [ethyl acetate/toluene/petroleum ether; 3:5:10]. FTIR (KBr), ν (cm^{-1}): 1680 (C═O of carbonyl), 1740 (C═O ester), 3459 (C═O) association of the amide-linked carbonyl group. ^{1}H NMR (500 MHz, $CDCl_3$, δ): 1.29 (t, 3*H*, $-COOCH_2CH_3$), 3.15 (dd, 1*H*, CHA, JAB = 17.5 Hz, JAX = 7 Hz), 3.75 (dd, 1*H*, CHB, JBA = 17.5 Hz, JBX = 6 Hz), 4.23 (t, 1*H*, CHX), 4.28 (S, 2*H*, $-CH_2$), 4.67 (q, 2*H*, $-COOCH_2CH_3$), 6.92(d, 1*H*, arom), 7.06 (t, 1*H*, H8, arom), 7.26 (t, 1*H*, H9, arom ring), 7.36(d, 1*H*, arom), 7.43 (d, 2*H*, aromatic), 7.89(d, 2*H*, aromatic). ^{13}C NMR (100 MHz,$CDCl_3$ -d_6, δ, ppm): δ = 13.85, δ = 37.30, δ = 38.08, 47.61, δ = 61.81, δ = 117.19,δ = 123.02,δ = 124.12, δ = 127.79, δ = 128.86, δ = 129.08(2C), δ = 129.74(2C), δ = 134.75, δ = 139.00, δ = 140.04, δ = 166.95, δ = 168.27, δ = 194.76. FAB-MS(*m*/*z*): 448 [M^+], 449 [M^+ + 1]. Molecular formula calculation was based on elemental analysis for the $C_{20}H_{18}BrNO_4S$: C = 53.58, H = 4.05, Br = 17.82, N = 3.12, O = 14.27, S = 7.15. Found: C = 53.48, H = 4.15, Br = 17.72, N = 3.02, O = 14.47, S = 7.35.

4.5. Biological Assays. *4.5.1. Cell Lines and Cell Culture.* The breast cancer cell line MCF-7 was obtained from the National Centre for Cell Science in Pune, India, for evaluating the in vitro anticancer potential of the compounds. Using modified Dulbecco Eagle's medium, six-walled cultural plates were used to culture the cells. In addition to 95% air condition and 5% CO_2, 10% fetal bovine serum was added at a temperature of 37 °C.

4.5.1.1. Investigation of Antiproliferative Activity by the MTT Assay against MCF-7. This method determines in vitro cytotoxic potential of compounds by assessing their inhibition activity against the MCF-7 breast cancer cell line. A 96-well plate with flat bottom was used for cell plating. Fresh media replaced growth media, after the cells got affixed to the plate, and incubated for 24 h with a series of dilutions (0.25, 0.5, 1, 2, 4, 8 μM) of compounds (**2a−f** and **3a−d**). Untreated cells acted as a control. To the plates of respective concentrations, phosphate-buffered saline having a concentration of 5 mg mL^{-1} was supplemented to 20 μL of MTT. For 4 h, it was

https://doi.org/10.1021/acsomega.2c07153
ACS Omega 2023, 8, 6650−6662

again incubated for facilitating the formation of formazan crystals. After dissolving these crystals in 200 μL of DMSO, carefully media from each well were drawn out, and then the media were further well shaken for 15 min to completely dissolve it. With the help of a microplate reader (Bio-Rad), at 570 nm, the optical density was computed for the solution. All of the experiments were accomplished in triplicates, and the viable cell average was determined. Using the formula used by Abdellatif et al.,[45] the percentage cell viability was calculated as follows

$$\text{cell viability}(\%) = \frac{(\text{optical density of the sample} - \text{optical density of control})}{\text{optical density of control}} \times 100$$

Prism software was used for plotting the graph b/w the cell viability and dilutions.

4.5.1.2. Analysis of the Cell Cycle. In PBS + 2% FBSS, a mono cell suspension was formed after harvesting the cells. They were then resuspended at 3−6 × 10^6 cells per mL after the MCF-7 cells were washed and spun at 300× *g* for 5 min. In a V-bottomed tube, an aliquant of 500 μL cells was drawn in 15 mL of polypropylene and was affixed with 70% ice-cold ethanol at 4 °C overnight. The cells were stained for 30 min with a propidium iodide solution after they were incubated with 50 μL of Rnase (10 μg m^{L-1}) at 37 °C for 1 h. Using BD FACS Diva 8.0.2 software (BD Biosciences-US), at 488 nm, the intensity of fluorescence was observed by carrying out flow cytometry.[46] For analysis of the cell cycle, all of the experiments were carried out in triplicate.

4.5.1.3. Wound Healing Assay. For compound **2c**, this assay was carried out by the reported method.[47] MCF-7 cell lines (1 × 10^5 cells per well) in 12-well plates were cultured for 24 h. The convergent monolayer was scratched by a P10-sterilized pipette tip. PBS was taken to wash the cell monolayer, and at 37 °C, it was again maintained with fresh media for removing the detached cells. Compound **2c** and compound-free solution at respective IC_{50} concentrations were treated with the MCF-7 cells. After treatment, a phase contrast microscope was used to capture images at 0 and 24 h; when across the wound, the migrated cells were identified. Comparative to the initial scratch, the percentage of wound closure can be calculated as follows

$$\text{wound closure}(\%) = \frac{(\text{area of wound } (t = 0\text{ h}) - \text{area of wound } (t = 24\text{ h}))}{\text{area of wound } (t = 0\text{ h})} \times 100$$

4.5.2. In Vitro VEGFR2 Kinase Assay. The effect of synthesized benzothiazinones and their acetate derivatives on VEGFR2 kinase was examined with the Alpha Screen system (Perkin Elmer). The kinase activity of VEGFR2 was measured by an antiphosphotyrosine antibody.[48] Enzyme reactions were carried out in 50 mM Tris-HCl (pH 7.5), 5 mM $MnCl_2$, 5 mM $MgCl_2$, 0.01% Tween-20, and 2 mM dithiothreitol containing 10 μM ATP, 0.1 μg/mL biotinylated poly-GluTyr (4:1), and 0.1 nM VEGFR2. The enzyme and tested compounds were incubated for 5 min at room temperature, prior to the catalytic initiation with ATP, with final concentrations ranging from 0 to 300 μg/mL; 25 μL of 100 mM ethylenediaminetetraacetic acid, 10 μg/mL α Screen streptavidin donor beads, and 10 μg/mL acceptor beads were added to 62.5 mM 4-(2hydroxyethyl)-1-piperazine ethanesulfonic acid pH 7.4, 250 mM NaCl, and 0.1% bovine serum albumin to quench the reactions. The plate was read by the ELISA Reader (Perkin Elmer) after being incubated in the dark for 10 h. The wells containing the substrate and enzyme (without compounds) were used as reaction control. As a basal control, biotinylated poly-GluTyr (4:1) and the enzyme devoid of ATP were employed in the wells. The percentage of inhibition was calculated from the concentration inhibition response curve, by comparing the compound treated to control incubations, and the test compound's 50% inhibitory concentration (IC_{50}) was calculated. The data were then compared to those obtained using sorafenib (Sigma-Aldrich), a standard VEGFR2 inhibitor.

4.5.3. Investigation of Anti-Inflammatory Activity Using the HRBC Membrane Stabilization Assay. The human red blood cell (HRBC) membrane stabilization assay was applied for investigating the anti-inflammatory potential of the compounds, which was developed by Shinde et al.[49] and altered by Sikder et al.[50] The blood of an adult normal female who had not consumed contraceptive or anti-inflammatory medicines in past two weeks, was taken. With the equivalent volume of Alsever's solution volume (0.42% NaCl in water, 2% dextrose, 0.8% sodium citrate, and 0.05% citric acid), the blood was mixed. For another 10 min, the mixture was centrifuged at 3000 rpm and with isosaline solution three times (0.9%, pH 7.2), the cells were washed, and then the supernatant was removed. Mixing 1 mL of phosphate buffer (pH 7.4), 2 mL of a solution of hyposaline (0.36%), and 0.5 mL of a suspension of HRBC (10% v/v), the assay mixture was made by taking 1 mg of every drug or standard, i.e., diclofenac sodium, of varying concentrations, i.e., (125, 250, and 500 μg/mL). Phosphate buffer was used as blank and dimethyl sulfoxide as control. The mixtures were centrifuged at 3000 rpm after incubating for 30 min at 37 °C. Spectrophotometrically at 560 nm, the content of hemoglobin in the supernatant solution was evaluated. With three replicates, 12 treatments were applied. In the presence of DMSO, the percentage of hemolysis was considered as 100%. The percent stabilization of the membrane was determined using the following formula[51]

$$\text{percentage of stabilization} = \frac{\text{abs (control)} - \text{abs (sample)}}{\text{abs (control)}} \times 100$$

4.5.4. Statistical Analysis. The mean ± standard deviation (SD) was presented as the data from individual groups. One-way ANOVA was used for statistical analysis for both anti-inflammatory and MTT assays, and *P* values <0.05 were regarded as statistically important. Values are taken as triplicate from three minimum independent experiments by the mean ± SE of samples. By linear regression studies, in vitro antiproliferative potential was indicated as IC_{50}. For examining the data of the cell cycle and wound healing assay, a multiple *t*-test was performed. GraphPad Prism 8.4 was used to perform statistical analysis.

4.6. In Silico Studies. *4.6.1. Molecular Docking.* Using Schrödinger 9.6 Maestro version software, molecular docking studies for newly synthesized benzothiazinones (**2a−f**) and their acetate derivatives (**3a−d**) were carried out at the molecular level in the VEGFR2 kinase receptor (PDB ID: 6GQO) for understanding the binding mode of these compounds. By the application of LigPrep, the ligands were prepared for docking, and in the 3D format, they were sketched by the build panel. From the protein data bank (PDB ID: 6GQO), the protein for the docking study was taken and

https://doi.org/10.1021/acsomega.2c07153
ACS Omega 2023, 8, 6650−6662

prepared using the protein preparation wizard by adding hydrogen and removing the solvent, and in the presence of bound ligands (F82), further minimization was done. Using the cocrystallized bound ligand, grids for molecular docking were generated, and the reference ligands (F82) were redocked in the protein catalytic site, showing that they occupy a similar binding pocket with a root mean square deviation (RMSD) of 0.715 A, which further supported the protocol of docking. By applying Glide extra-precision (XP) mode, compounds (**2a−f** and **3a−d**) were docked until three poses were saved per molecule.[43,44]

4.6.2. GBSA/MM Study. By implementing energy calculations in the prime module of the Schrödinger molecular modeling package from GBSA/MM analysis, free energies of binding for compound **2c** and the cocrystalized ligand (F82) with 6GQO were carried out. Free energies of binding of respective structures were evaluated using the OPLS3 force field and the VSGB 2.0 model of solvation by selecting complex structures.[43]

■ ASSOCIATED CONTENT

Supporting Information

The Supporting Information is available free of charge at https://pubs.acs.org/doi/10.1021/acsomega.2c07153.

Mass; ^{1}H NMR; and ^{13}C spectra of synthesized compounds (PDF)

■ AUTHOR INFORMATION

Corresponding Authors

Sameena Bano − *Department of Computer Science and Engineering, School of Engineering Sciences and Technology, Jamia Hamdard (Hamdard University), New Delhi 110062, India*; Phone: +919210707636; Email: sameenabano01@gmail.com

Kalim Javed − *Department of Chemistry, School of Chemical and Life Sciences, Jamia Hamdard (Hamdard University), New Delhi 110062, India*; orcid.org/0000-0002-5036-5230; Phone: +919873463272; Email: kjaved@jamiahamdard.ac.in

Authors

Farhat Ramzan − *Department of Chemistry, School of Chemical and Life Sciences, Jamia Hamdard (Hamdard University), New Delhi 110062, India*

Syed Ayaz Nabi − *Department of Chemistry, School of Chemical and Life Sciences, Jamia Hamdard (Hamdard University), New Delhi 110062, India*

Mehak Saba Lone − *Department of Chemistry, School of Chemical and Life Sciences, Jamia Hamdard (Hamdard University), New Delhi 110062, India*

Khalid Imtiyaz − *Department of Biosciences, Genome biology lab, Jamia Millia Islamia, New Delhi 110025, India*; orcid.org/0000-0003-2854-5857

Laraib Urooj − *Department of Biosciences, Genome biology lab, Jamia Millia Islamia, New Delhi 110025, India*

Vishakha Vishakha − *Central European Institute of Technology, Brno University of Technology, Brno 61200, Czech Republic*

Kalicharan Sharma − *Department of Pharmaceutical Chemistry, Delhi Pharmaceutical Sciences and Research University Pushpvihar, New Delhi 110017, India*

M. Moshahid A. Rizvi − *Department of Biosciences, Genome biology lab, Jamia Millia Islamia, New Delhi 110025, India*

Syed Shafi − *Department of Chemistry, School of Chemical and Life Sciences, Jamia Hamdard (Hamdard University), New Delhi 110062, India*; orcid.org/0000-0001-7657-0630

Mohammed Samim − *Department of Chemistry, School of Chemical and Life Sciences, Jamia Hamdard (Hamdard University), New Delhi 110062, India*; orcid.org/0000-0003-1667-8572

Complete contact information is available at: https://pubs.acs.org/10.1021/acsomega.2c07153

Author Contributions

F.R.: investigation, writing—original draft, methodology, formal analysis, and review. S.A.N., M.S.L., K.I., L.U., V.V., and M.M.A.R.: methodology and review. K.S.: software, methodology, and review. M.S. and S.S.: review and supervision. S.B.: writing—original draft, methodology, and review. K.J.: conceptualization, writing—original draft, investigation, methodology, and supervision.

Notes

The authors declare no competing financial interest.

■ ACKNOWLEDGMENTS

The authors convey their profound sense of appreciation to IIT, Delhi, for their Central Research Facility, JMI, New Delhi, for providing Central Instrumentation Facility, and JNU, New Delhi, for providing their Advanced Instrumentation Research Facility to carry out spectral analysis. F.R. is thankful to ICMR, New Delhi for Senior Research Fellowship no. 3/1/3(4)/Endo-fellowship/22-NCD-III.

■ REFERENCES

(1) Shewach, D. S.; Kuchta, R. D. Introduction to Cancer Chemotherapeutics. *Chem. Rev.* **2009**, *109*, 2859−2861.

(2) Taher, A. T.; Mohammed, L. W. Synthesis of New 1,3,4-Benzotriazepin-5-One Derivatives and Their Biological Evaluation as Antitumor Agents. *Arch. Pharmacal. Res.* **2013**, *36*, 684−693.

(3) Rathore, P.; Yaseen, S.; Ovais, S.; Bashir, R.; Yaseen, R.; Hameed, A. D.; Samim, M.; Gupta, R.; Hussain, F.; Javed, K. Synthesis and Evaluation of Some New Pyrazoline Substituted Benzenesulfonylureas as Potential Antiproliferative Agents. *Bioorg. Med. Chem. Lett.* **2014**, *24*, 1685−1691.

(4) Bashandy, M. S.; Alsaid, M. S.; Arafa, R. K.; Ghorab, M. M. Design, Synthesis and Molecular Docking of Novel N,N-Dimethylbenzenesulfonamide Derivatives as Potential Antiproliferative Agents. *J. Enzyme Inhib. Med. Chem.* **2014**, *29*, 619−627.

(5) Iorns, E.; Drews-Elger, K.; Ward, T. M.; Dean, S.; Clarke, J.; Berry, D.; El Ashry, D.; Lippman, M. A New Mouse Model for the Study of Human Breast Cancer Metastasis. *PLoS One* **2012**, *7*, No. e47995.

(6) Ferlay, J.; Colombet, M.; Soerjomataram, I.; Mathers, C.; Parkin, D. M.; Piñeros, M.; Znaor, A.; Bray, F. Estimating the Global Cancer Incidence and Mortality in 2018: GLOBOCAN Sources and Methods. *Int. J. Cancer* **2019**, *144*, 1941−1953.

(7) Sibuh, B. Z.; Khanna, S.; Taneja, P.; Sarkar, P.; Taneja, N. K. Molecular Docking, Synthesis and Anticancer Activity of Thiosemicarbazone Derivatives against MCF-7 Human Breast Cancer Cell Line. *Life Sci.* **2021**, *273*, No. 119305.

(8) Sharma, G. N.; Dave, R.; Sanadya, J.; Sharma, P.; Sharma, K. K. Various Types and Management of Breast Cancer: An Overview. *J. Adv. Pharm. Technol. Res.* **2010**, *1*, 109−126.

(9) Rayburn, E. R.; Ezell, S. J.; Zhang, R. Anti-Inflammatory Agents for Cancer Therapy. *Mol. Cell. Pharmacol.* **2009**, *1*, 29−43.

(10) Fujiwara, N.; Kobayashi, K. Macrophages in Inflammation. *Curr. Drug Targets: Inflammation Allergy* **2005**, *4*, 281−286.
(11) Duque, G. A.; Descoteaux, A. Macrophage Cytokines: Involvement in Immunity and Infectious Diseases. *Front. Immunol.* **2014**, *5*, No. 491.
(12) Boelsterli, U. A.Mechanisms Underlying the Hepatotoxicity of Nonsteroidal Antiinflammatory Drugs. In *Drug-Induced Liver Disease*; Elsevier, 2013; pp 343−367.
(13) Bhala, N.; Emberson, J.; Merhi, A.; Abramson, S.; Arber, N.; Baron, J. A.; Bombardier, C.; Cannon, C.; Farkouh, M. E.; FitzGerald, G. A.; Goss, P.; Halls, H.; Hawk, E.; Hawkey, C.; Hennekens, C.; Hochberg, M.; Holland, L. E.; Kearney, P. M.; Laine, L.; Lanas, A.; Lance, P.; Laupacis, A.; Oates, J.; Patrono, C.; Schnitzer, T. J.; Solomon, S.; Tugwell, P.; Wilson, K.; Wittes, J.; Baigent, C. Vascular and Upper Gastrointestinal Effects of Non-Steroidal Anti-Inflammatory Drugs: Meta-Analyses of Individual Participant Data from Randomised Trials. *Lancet* **2013**, *382*, 769−779.
(14) Abdel-Mohsen, H. T.; Abd El-Meguid, E. A.; El Kerdawy, A. M.; Mahmoud, A. E. E.; Ali, M. M. Design, Synthesis, and Molecular Docking of Novel 2-Arylbenzothiazole Multiangiokinase Inhibitors Targeting Breast Cancer. *Arch. Pharm.* **2020**, *353*, No. 1900340.
(15) Cecchetti, V.; Fravolini, A.; Fringuelli, R.; Mascellani, G.; Pagella, P.; Palmioli, M.; Segre, G.; Terni, P. Quinolonecarboxylic Acids. 2. Synthesis and Antibacterial Evaluation of 7-Oxo-2,3-Dihydro-7H-Pyrido[1,2,3-de][1,4]Benzothiazine-6-Carboxylic Acids. *J. Med. Chem.* **1987**, *30*, 465−473.
(16) Armenise, D.; Trapani, G.; Arrivo, V.; Morlacchi, F. Preparation of Potentially Bioactive Aza and Thiaza Polycyclic Compounds Containing a Bridgehead Nitrogen Atom Synthesis and Antimicrobial Activity of Some Pyrrolo[1,2,3-de]-1,4-Benzothiazines. *Farmaco* **1991**, *46*, 1023−1032.
(17) Armenise, D.; Trapani, G.; Stasi, F.; Morlacchi, F. Research on Potentially Bioactive Aza and Thiaza Polycyclic Compounds Containing a Bridgehead Nitrogen Atom. Synthesis and Antimicrobial Activity of Some Pyrrolo[1,2,3-de]-1,4-Benzothiazines, Part 2. *Arch. Pharm.* **1998**, *331*, 54−58.
(18) Schiaffella, F.; Macchiarulo, A.; Milanese, L.; Vecchiarelli, A.; Costantino, G.; Pietrella, D.; Fringuelli, R. Design, Synthesis, and Microbiological Evaluation of New Candida Albicans CYP51 Inhibitors. *J. Med. Chem.* **2005**, *48*, 7658−7666.
(19) Armenise, D.; Muraglia, M.; Florio, M. A.; De Laurentis, N.; Rosato, A.; Carrieri, A.; Corbo, F.; Franchini, C. 4H-1,4-Benzothiazine, Dihydro-1,4-Benzothiazinones and 2-Amino-5-Fluorobenzenethiol Derivatives: Design, Synthesis and in Vitro Antimicrobial Screening. *Arch. Pharm* **2012**, *345*, 407−416.
(20) Zhang, P.; Hu, H.-R.; Bian, S.-H.; Huang, Z.-H.; Chu, Y.; Ye, D.-Y. Design, Synthesis and Biological Evaluation of Benzothiazepinones (BTZs) as Novel Non-ATP Competitive Inhibitors of Glycogen Synthase Kinase-3β (GSK-3β). *Eur. J. Med. Chem.* **2013**, *61*, 95−103.
(21) Zhang, P.; Li, S.; Gao, Y.; Lu, W.; Huang, K.; Ye, D.; Li, X.; Chu, Y. Novel Benzothiazinones (BTOs) as Allosteric Modulator or Substrate Competitive Inhibitor of Glycogen Synthase Kinase 3β (GSK-3β) with Cellular Activity of Promoting Glucose Uptake. *Bioorg. Med. Chem. Lett.* **2014**, *24*, 5639−5643.
(22) Grandolini, G.; Perioli, L.; Ambrogi, V. Synthesis of Some New 1, 4-Benzothiazine and 1, 5-Benzothiazepine Tricyclic Derivatives with Structural Analogy with TIBO and Their Screening for Anti-HIV Activity. *Eur. J. Med. Chem.* **1999**, *34*, 701−709.
(23) Kamel, M. M.; Ali, H. I.; Anwar, M. M.; Mohamed, N. A.; Soliman, A. M. Synthesis, Antitumor Activity and Molecular Docking Study of Novel Sulfonamide-Schiff's Bases, Thiazolidinones, Benzothiazinones and Their C-Nucleoside Derivatives. *Eur. J. Med. Chem.* **2010**, *45*, 572−580.
(24) Chandran, M.; Renuka, J.; Sridevi, J. P.; Pedgaonkar, G. S.; Asmitha, V.; Yogeeswari, P.; Sriram, D. Benzothiazinone-Piperazine Derivatives as Efficient *Mycobacterium Tuberculosis* DNA Gyrase Inhibitors. *Int. J. Mycobact.* **2015**, *4*, 104−115.
(25) Li, J.; Fan, X.; Deng, J.; Liang, Y.; Ma, S.; Lu, Y.; Zhang, J.; Shi, T.; Tan, W.; Wang, Z. Design and Synthesis of 1,3-Benzothiazinone Derivatives as Potential Anti-Inflammatory Agents. *Bioorg. Med. Chem.* **2020**, *28*, No. 115526.
(26) Gao, Y.; Ye, D.-Y.; Zhou, W.-C.; Chu, Y. The Discovery of Novel Benzothiazinones as Highly Selective Non-ATP Competitive Glycogen Synthase Kinase 3β Inhibitors for the Treatment of Ovarian Cancer. *Eur. J. Med. Chem.* **2017**, *135*, 370−381.
(27) Khoshneviszadeh, M.; Ghahremani, M. H.; Foroumadi, A.; Miri, R.; Firuzi, O.; Madadkar-Sobhani, A.; Edraki, N.; Parsa, M.; Shafiee, A. Design, Synthesis and Biological Evaluation of Novel Anti-Cytokine 1,2,4-Triazine Derivatives. *Bioorg. Med. Chem.* **2013**, *21*, 6708−6717.
(28) Kumar, R.; Sirohi, T. S.; Singh, H.; Yadav, R.; Roy, R. K.; Chaudhary, A.; Pandeya, S. N. 1,2,4-Triazine Analogs as Novel Class of Therapeutic Agents. *Mini-Rev. Med. Chem.* **2014**, *14*, 168−207.
(29) Karoli, T.; Becker, B.; Zuegg, J.; Möllmann, U.; Ramu, S.; Huang, J. X.; Cooper, M. A. Identification of Antitubercular Benzothiazinone Compounds by Ligand-Based Design. *J. Med. Chem.* **2012**, *55*, 7940−7944.
(30) Fenner, H. Comparative Biochemical Pharmacology of the Oxicams. *Scand. J. Rheumatol.* **1987**, *16*, 97−101.
(31) Young, R. Inhibitors of 5-Lipoxygenase: A Therapeutic Potential yet to Be Fully Realized. *Eur. J. Med. Chem.* **1999**, *34*, 671−685.
(32) Beryozkina, T. V.; Kolos, N. N.; Orlov, V. D.; Zubatyuk, R. I.; Shishkin, O. V. 2-(2-Aryl-2-Oxoethyl)-4H-Benzo-1,4-Thiazin-3-Ones as Products of the Reaction of 2-Aminothiophenol with β-Aroylacrylic Acids. *Phosphorus, Sulfur Silicon Relat. Elem.* **2004**, *179*, 2153−2162.
(33) Khan, M. S. Y.; Siddiqui, A. A. Synthesis and Antiinflammatory Activity of Some 6-Aryl-2, 3, 4, 5-Tetrahydro-3-Pyridazinones. *Indian J. Chem.* **2000**, *39B*, 614−619.
(34) Khan, M. S. Y.; Husain, A.; Sharma, S. Studies on Butenolides: 2-Arylidene-4-(Substituted Aryl) but-3-En-4-Olides—Synthesis, Reactions and Biological Activity. *Indian J. Chem.* **2002**, *41B*, 2160−2171.
(35) Mosmann, T. Rapid Colorimetric Assay for Cellular Growth and Survival: Application to Proliferation and Cytotoxicity Assays. *J. Immunol. Methods* **1983**, *65*, 55−63.
(36) Dhahagani, K.; Kumar, S. M.; Chakkaravarthi, G.; Anitha, K.; Rajesh, J.; Ramu, A.; Rajagopal, G. Synthesis and Spectral Characterization of Schiff Base Complexes of Cu(II), Co(II), Zn(II) and VO(IV) Containing 4-(4-Aminophenyl)Morpholine Derivatives: Antimicrobial Evaluation and Anticancer Studies. *Spectrochim. Acta, Part A* **2014**, *117*, 87−94.
(37) Nunez, R. DNA Measurement and Cell Cycle Analysis by Flow Cytometry. *Curr. Issues Mol. Biol.* **2001**, *3*, 67−70.
(38) Jonkman, J. E. N.; Cathcart, J. A.; Xu, F.; Bartolini, M. E.; Amon, J. E.; Stevens, K. M.; Colarusso, P. An Introduction to the Wound Healing Assay Using Live-Cell Microscopy. *Cell Adhes. Migr.* **2014**, *8*, 440−451.
(39) Ashtari, N.; Jiao, X.; Rahimi-Balaei, M.; Amiri, S.; Mehr, S. E.; Yeganeh, B.; Marzban, H. Lysosomal Acid Phosphatase Biosynthesis and Dysfunction: A Mini Review Focused on Lysosomal Enzyme Dysfunction in Brain. *Curr. Mol. Med.* **2016**, *16*, 439−446.
(40) Basli, A.; Sonia, T.; Nawel, I.; Bachra, K.; Khodir, M. In-Vitro Antioxidant and Anti-Inflammatory Activities of Peel and Peeled Fruits Citrus Limon. *Curr. Nutr. Food Sci.* **2016**, *12*, 279−287.
(41) Chowdhury, A.; Azam, S.; Jainul, M. A.; Faruq, K. O.; Islam, A. Antibacterial Activities and In Vitro Anti-Inflammatory (Membrane Stability) Properties of Methanolic Extracts of *Gardenia Coronaria* Leaves. *Int. J. Microbiol.* **2014**, *2014*, No. 410935.
(42) Vane, J. R.; Botting, R. M. New Insights into the Mode of Action of Anti-Inflammatory Drugs. *Inflammation Res.* **1995**, *44*, 1−10.
(43) Potashman, M. H.; Bready, J.; Coxon, A.; DeMelfi, T. M. J.; DiPietro, L.; Doerr, N.; Elbaum, D.; Estrada, J.; Gallant, P.; Germain, J.; Gu, Y.; Harmange, J.-C.; Kaufman, S. A.; Kendall, R.; Kim, J. L.; Kumar, G. N.; Long, A. M.; Neervannan, S.; Patel, V. F.; Polverino,

https://doi.org/10.1021/acsomega.2c07153
ACS Omega 2023, 8, 6650−6662

A.; Rose, P.; van der Plas, S.; Whittington, D.; Zanon, R.; Zhao, H. Design, Synthesis, and Evaluation of Orally Active Benzimidazoles and Benzoxazoles as Vascular Endothelial Growth Factor-2 Receptor Tyrosine Kinase Inhibitors. *J. Med. Chem.* **2007**, *50*, 4351−4373.
(44) Sharma, K.; Shrivastava, A.; Mehra, R. N.; Deora, G. S.; Alam, M. M.; Zaman, M. S.; Akhter, M. Synthesis of Novel Benzimidazole Acrylonitriles for Inhibition of Plasmodium Falciparum Growth by Dual Target Inhibition. *Arch. Pharm.* **2018**, *351*, No. 1700251.
(45) Abdellatif, K. R. A.; Belal, A.; El-Saadi, M. T.; Amin, N. H.; Said, E. G.; Hemeda, L. R. Design, Synthesis, Molecular Docking and Antiproliferative Activity of Some Novel Benzothiazole Derivatives Targeting EGFR/HER2 and TS. *Bioorg. Chem.* **2020**, *101*, No. 103976.
(46) Liu, J.; He, Y.; Zhang, D.; Cai, Y.; Zhang, C.; Zhang, P.; Zhu, H.; Xu, N.; Liang, S. In Vitro Anticancer Effects of Two Novel Phenanthroindolizidine Alkaloid Compounds on Human Colon and Liver Cancer Cells. *Mol. Med. Rep.* **2017**, *16*, 2595−2603.
(47) Imran, M.; Iqubal, M. K.; Imtiyaz, K.; Saleem, S.; Mittal, S.; Rizvi, M. M. A.; Ali, J.; Baboota, S. Topical Nanostructured Lipid Carrier Gel of Quercetin and Resveratrol: Formulation, Optimization, in Vitro and Ex Vivo Study for the Treatment of Skin Cancer. *Int. J. Pharm.* **2020**, *587*, No. 119705.
(48) El-Helby, A. A.; Sakr, H.; Eissa, I. H.; Al-Karmalawy, A. A.; El-Adl, K. Benzoxazole/Benzothiazole -Derived VEGFR-2 Inhibitors: Design, Synthesis, Molecular Docking, and Anticancer Evaluations. *Arch. Pharm.* **2019**, *352*, No. 1900178.
(49) Shinde, U. A.; Phadke, A. S.; Nair, A. M.; Mungantiwar, A. A.; Dikshit, V. J.; Saraf, M. N. Membrane Stabilizing Activity—a Possible Mechanism of Action for the Anti-Inflammatory Activity of *Cedrus Deodara* Wood Oil. *Fitoterapia* **1999**, *70*, 251−257.
(50) Rahman, M. S.; Rashid, M. A.; Sikder, A. A.; Rahman, A.; Kaisar, M. A.; Hasan, C. M. In Vitro Antioxidant, Reducing Power, Free Radical Scavenging and Membrane Stabilizing Activities of Seeds of *Syzygium Cumini*. *Lat. Am. J. Pharm.* **2011**, *30*, 781−785.
(51) León, J. A.; Santisteban, A. G.; Fuentes, D. P.; Puebla, Y. G.; Rodriguez, E. T. In Vitro Anti-Inflammatory Activity of Aqueous, Ethanolic and Ethereal Extracts of Rhizomes, Leaves and Stems of *Anredera Vesicaria*. *J. Anal. Pharm. Res.* **2018**, *7*, 459−461.

https://doi.org/10.1021/acsomega.2c07153
ACS Omega 2023, 8, 6650−6662